# Bendadaite, a new iron arsenate mineral of the arthurite group

U. Kolitsch[1,2,*], D. Atencio[3], N. V. Chukanov[4], N. V. Zubkova[5], L. A. D. Menezes Filho[6],
J. M. V. Coutinho[3], W. D. Birch[7], J. Schlüter[8], D. Pohl[9], A. R. Kampf[10], I. M. Steele[11], G. Favreau[12],
L. Nasdala[2], S. Möckel[13], G. Giester[2] and D. Yu. Pushcharovsky[5]

[1]  Mineralogisch-Petrographische Abt., Naturhistorisches Museum, Burgring 7, A-1010 Wien, Austria
[2]  Institut für Mineralogie und Kristallographie, Universität Wien, Althanstr. 14, A-1090 Wien, Austria
[3]  Instituto de Geociências, Universidade de São Paulo, Rua do Lago, 562, 05508−080, São Paulo, SP, Brazil
[4]  Institute of Problems of Chemical Physics, 142432 Chernogolovka, Moscow Oblast, Russia
[5]  M.V. Lomonosov Moscow State University, Faculty of Geology, Vorobjovy Gory, 119899 Moscow, Russia
[6]  Instituto de Geociências, Universidade Federal de Minas Gerais, Av. Antônio Carlos, 6627, 3127–901, Belo
     Horizonte, MG, Brazil
[7]  Department of Mineralogy, Museum Victoria, GPO Box 666, Melbourne, Victoria 3001, Australia
[8]  Mineralogisches Museum, Universität Hamburg, Grindelallee 48, D-20146 Hamburg, Germany
[9]  Mineralogisch-Petrographisches Institut, Universität Hamburg, Grindelallee 48, D-20146 Hamburg, Germany
[10] Mineral Sciences Department, Natural History Museum of Los Angeles County, 900 Exposition Blvd., Los
     Angeles, CA 90007, USA
[11] Senior Research Associate, Department of Geophysical Sciences, University of Chicago, 5734 S. Ellis Avenue,
     Chicago IL 60637, USA
[12] 421 av. Jean Monnet, F-13090 Aix-en-Provence, France
[13] Neudorfer Str. 18, D-09629 Burkersdorf, Germany

## ABSTRACT

Bendadaite, ideally $Fe^{2+}Fe_2^{3+}(AsO_4)_2(OH)_2 \cdot 4H_2O$, is a new member of the arthurite group. It was found as a weathering product of arsenopyrite on a single hand specimen from the phosphate pegmatite Bendada, central Portugal (type locality). Co-type locality is the granite pegmatite of Lavra do Almerindo (Almerindo mine), Linópolis, Divino das Laranjeiras county, Minas Gerais, Brazil. Further localities are the Veta Negra mine, Copiapó province, Chile; Oumlil-East, Bou Azzer district, Morocco; and Pira Inferida yard, Fenugu Sibiri mine, Gonnosfanadiga, Medio Campidano Province, Sardinia, Italy.

Type bendadaite occurs as blackish green to dark brownish tufts (<0.1 mm long) and flattened radiating aggregates, in intimate association with an intermediate member of the scorodite–mansfieldite series. It is monoclinic, space group $P2_1/c$, with $a$ = 10.239(3) Å, $b$ = 9.713(2) Å, $c$ = 5.552(2) Å, $\beta$ = 94.11(2)°, $V$ = 550.7(2) Å$^3$, $Z$ = 2. Electron-microprobe analysis yielded (wt.%): CaO 0.04, MnO 0.03, CuO 0.06, ZnO 0.04, $Fe_2O_3$ (total) 43.92, $Al_2O_3$ 1.15, $SnO_2$ 0.10, $As_2O_5$ 43.27, $P_2O_5$ 1.86, $SO_3$ 0.03. The empirical formula is $(Fe_{0.52}^{2+}Fe_{0.32}^{3+}\square_{0.16})_{\Sigma1.00}(Fe_{1.89}^{3+}Al_{0.11})_{\Sigma2.00}(As_{1.87}P_{0.13})_{\Sigma2.00}O_8(OH)_{2.00} \cdot 4H_2O$, based on 2(As,P) and assuming ideal 8O, 2(OH), $4H_2O$ and complete occupancy of the ferric iron site by $Fe^{3+}$ and Al. Optically, bendadaite is biaxial, positive, $2V_{est.}$ = 85±4°, $2V_{calc.}$ = 88°, with $\alpha$ 1.734(3), $\beta$ 1.759(3), $\gamma$ 1.787(4). Pleochroism is medium strong: $X$ pale reddish brown, $Y$ yellowish brown, $Z$ dark yellowish brown; absorption $Z > Y > X$, optical dispersion weak, $r > v$. Optical axis plane is parallel to (010), with $X$ approximately parallel to $a$ and $Z$ nearly parallel to c. Bendadaite has vitreous to sub-adamantine luster, is translucent and non-fluorescent. It is brittle, shows irregular fracture and a good cleavage parallel to {010}. $D_{meas.}$ 3.15±0.10 g/cm$^3$, $D_{calc.}$ 3.193 g/cm$^3$ (for the empirical formula). The five strongest powder diffraction lines [$d$ in Å (I)($hkl$)] are 10.22 (10)(100), 7.036 (8)(110), 4.250 (5)(111), 2.865 (4)($\bar{3}$11), 4.833 (3)(020,011). The $d$ spacings are very similar to those of its Zn analogue, ojuelaite. The crystal structure of bendadaite was solved and refined using a crystal from the co-type locality with the composition $(Fe_{0.95}^{2+}\square_{0.05})_{\Sigma1.00}(Fe_{1.80}^{3+}Al_{0.20})_{\Sigma2.00}(As_{1.48}P_{0.52})_{\Sigma2.00}O_8$ $(OH)_2 \cdot 4H_2O$ ($R$ = 1.6%), and confirms an arthurite-type atomic arrangement.

## Introduction

DURING a 1987 field trip to Portugal of members of the Institut für Mineralogie und Kristallchemie of the Universität Stuttgart, Germany, the student J. Argyrakis collected an arsenopyrite-bearing hand specimen on the dumps of the phosphate-bearing pegmatite at Bendada, central Portugal. A later, close inspection of the hand specimen by the senior author in about 1993 showed an unknown blackish green to dark brownish mineral forming tiny tufts on and near corroded, massive arsenopyrite. Detailed investigations of the very scarce material revealed the mineral to be a new hydrated iron arsenate mineral and a new end-member of the arthurite group. An original submission as a new mineral species in 1998 to the (then) Commission on New Minerals and Mineral Names (CNMMN) of the IMA (proposal 98-053) was put on hold due to inadequate electron microprobe data. Additional data were subsequently obtained from new finds of the mineral in Brazil, Chile and Morocco. After a resubmission of an improved proposal, including a crystal-structure analysis of a crystal from Brazil, and additional spectroscopic data, the description and name were approved by the Commission on New Minerals, Nomenclature and Classification (CNMNC), IMA, in 2007 (IMA 98-053a). The species is named after the type locality. The co-type locality is the granite pegmatite of Lavra do Almerindo (Almerindo mine), Linópolis, Divino das Laranjeiras county, Minas Gerais, Brazil. Bendadaite has also been found in the Veta Negra mine, Copiapó province, Chile, and Oumlil-East, Bou Azzer district, Morocco (as small Fe-dominant portions of some cobaltarthurite crystals; Kampf *et al.*, 2004; Kampf, 2005; Favreau and Dietrich, 2006), as well as Pira Inferida yard, Fenugu Sibiri mine, Gonnosfanadiga, Medio Campidano Province, Sardinia, Italy (M. Ciriotti, G. Blaß and W. Krause, pers. comm. with U. Kolitsch, 2007). The type material has been deposited in the collection of the Natural History Museum, Vienna, Austria (catalogue number N 8160). The co-type material has been deposited in the Museu de Geociências, Instituto de Geociências, Universidade de São Paulo, Brazil (catalogue number DR625).

## Occurrence and paragenesis

The bendadaite-bearing specimen was found on the dumps of the phosphate-bearing columbite-beryl pegmatite occurrence of Bendada near Guarda, province Beira Alta, central Portugal (Correia Neves, 1960; Rewitzer and Röschl, 1984). The geology and mineralogy of this occurrence were described by Schnorrer-Köhler and Rewitzer (1991). The pegmatite hand specimen consisted of iron-stained muscovite, K-feldspar, quartz, and large, irregular, super-ficially weathered masses of arsenopyrite. In the quartz matrix of polished sections, tiny, brassy grains of an unidentified Cu-Fe-Sn-sulphide and tiny, grey grains of an unidentified Cu-sulphide were observed. Yellowish grey to greenish grey, thin microcrystalline crusts of scorodite–mansfieldite cover the weathered arsenopyrite and narrow fissures. Very minor gypsum is also present as indistinct crusts on the scorodite–mansfieldite. Blackish green to dark brown bendadaite occurs in intimate association with scorodite–mansfieldite, and most of the bend-adaite is overgrown by the latter. This assemblage suggests that bendadaite was formed at about the same time as scorodite–mansfieldite. The scor-odite–mansfieldite crusts were identified by their X-ray powder pattern and optical properties. The refined unit-cell parameters, $a = 10.244(13)$, $b = 9.914(13)$, $c = 8.881(9)$ Å, place these crusts in the intermediate range of the solid-solution series (Allen *et al.*, 1948; Walenta, 1963; Dasgupta *et al.*, 1966; Dove and Rimstidt, 1985; Krause and Ettel, 1988). The refraction index, $\alpha$, of the crusts was found to be quite variable (1.710 to 1.730), even within tiny fragments. The outer zones of the crusts showed greater refraction indices and stronger pleochroism, thus indicating larger Fe contents. Very minor gypsum has been noted as colourless, skeletal, crystalline crusts on scorodite–mansfieldite and bendadaite. Seven thumbnail-sized specimens containing very small amounts of bendadaite could be recovered from the hand specimen; all of these small specimens constitute the type material.

At the co-type locality, Lavra do Almerindo (Almerindo mine), Linópolis, Divino das Laranjeiras county, Minas Gerais, Brazil, the species accompanying bendadaite are albite, muscovite, quartz, schorl, elbaite, löllingite,

scorodite, pharmacosiderite, saléeite and phosphuranylite.

At the Veta Negra mine, Copiapó province, Chile, bendadaite is accompanied by arsenopyrite, erythrite and pharmacosiderite, and, according to A. Molina (pers. comm. to J. Schlüter), also parasymplesite, karibibite, scorodite and 'limonite'. At Oumlil-East, Bou Azzer district, Morocco, bendadaite occurs as small Fe-dominant portions of some cobaltarthurite crystals (Kampf *et al.*, 2004; Kampf, 2005; Favreau and Dietrich, 2006). These crystals are found in an association containing karibibite, schneiderhöhnite, Co-bearing löllingite, parasymplesite, pharmacosiderite, scorodite and erythrite.

At the type locality, bendadaite has formed as a secondary (or low-*T*, late-hydrothermal) mineral with Fe and As derived from weathered arsenopyrite. The intimate association with scorodite−mansfieldite (type locality material) indicates formation at low pH and moderate to high Eh (Vink, 1996; Krause and Ettel, 1988; Dove and Rimstidt, 1985; Rimstidt and Dove, 1987). The assemblages at other localities indicated similar conditions of formation.

## Physical and optical properties

Type bendadaite occurs as blackish green to dark brownish tufts and, in narrow fissures, as radiating aggregates composed of elongate crystallites (Figs 1, 2). The elongation is parallel to [001]. No distinct single crystals or cleavage fragments could be found or isolated from the tufts. The length of the bendadaite tufts and the radius of the aggregates are commonly <0.1 mm; only on one specimen a maximum radius of ~0.2 mm is reached. Aggregates appear opaque to semi-translucent, but thin elongate cleavage plates are translucent and greenish brown. The streak is greenish yellow. The lustre is vitreous to subadamantine on cleavages, but dull on the surface of the hemispheres. The Mohs hardness is ~3. Bendadaite is brittle, its cleavage is good parallel to (010) and its fracture is irregular. The density, $3.15\pm0.10$ g/cm$^3$, was measured by suspension in heavy liquids; the large measurement error is a result of the small size of the aggregates used. The calculated density, using the empirical formula, is 3.193 g/cm$^3$ for Z = 2; the corresponding value for the co-type material is 3.155 g/cm$^3$ (based on the crystal-structure data). For the type material, the Gladstone-Dale compatibility index according to Mandarino (1981) is 0.035, i.e. 'excellent'. Bendadaite dissolves in hot dilute HCl or HNO$_3$ but not in cold acids. The solution gives a strong reaction for Fe$^{3+}$. Microchemical tests for ferrous iron (using Merckoquant 10.004, Merck, Germany) were also positive. The arsenate mineral may be easily mistaken for several dark greenish or dark brownish phosphates occurring in pegmatites. However, the association with weathered arsenopyrite (or löllingite), scorodite and pharmacosiderite may be a good indicator for its occurrence.
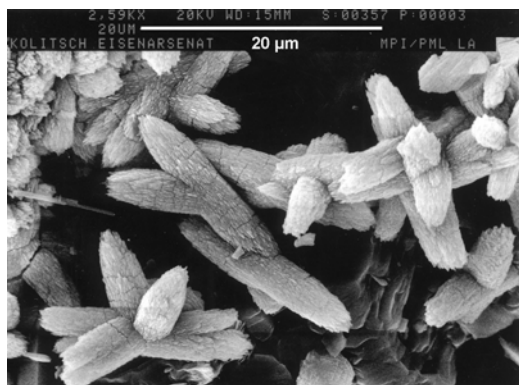


FIG. 1. SEM image of bendadaite tufts grown on scorodite−mansfieldite crusts (type material). The cracks seen in the tufts are obviously caused by dehydration in the vacuum of the SEM chamber.
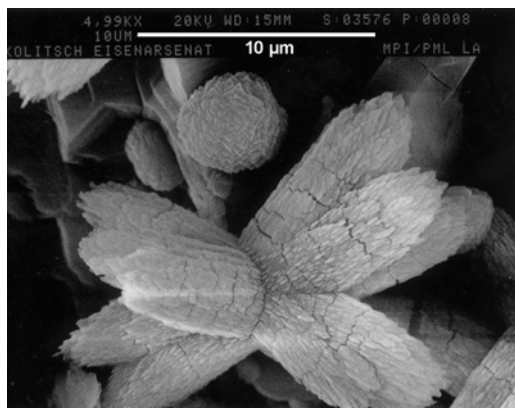


FIG. 2. Close-up SEM image of an intergrowth of bendadaite tufts (type material).

About seven thumbnail-sized specimens containing very small amounts of type bendadaite exist. Most of the bendadaite is overgrown by scorodite-mansfieldite crusts.

Co-type bendadaite from Brazil is also very scarce: it was found inside small cavities in albite, some decimeters away from a large block of löllingite. Only five hand-size specimens were found, and only one had a 5 mm-thick layer of elongated, tabular, dark greenish-brown bendadaite crystals (Fig. 3), partially coated with tufts of divergent, pale yellowish-green, acicular bendadaite crystals; the remaining four specimens contained globular to pellet-like aggregates of very pale yellowish-green acicular bendadaite crystals, measuring up to 0.3 mm, and were associated with spherical light grey clusters of scorodite crystals, over a matrix of corroded albite.

The Veta Negra (Chile) bendadaite specimens, collected by Messrs Arturo Molina and Maurizio Dini, show sprays of acicular straw yellow, yellow or golden brown crystals up to 1 mm in length. At the Pira Inferida yard (Italy), bendadaite was found by Mr Sergio Mascia. It forms small, golden-yellow, acicular crystals which are associated with olivenite in a void of a matrix containing Ni-Co sulphides; the locality is known for blocks containing nickeline, skutterudite, millerite and other Ni-Co sulphides, with the alteration products mimetite, scorodite(-mansfiel-

dite), olivenite and erythrite (M. Ciriotti and G. Blaß, pers. comm. to U. Kolitsch, 2007).

Optical properties were determined by the immersion method in white light. Since no single free-standing crystals were available in the type material, only platy elongated crystallites (cleavage fragments) could be used to determine the properties. The measured refractive indices are $\alpha$ 1.734(3), $\beta$ 1.759(3) and $\gamma$ 1.787(4). Bendadaite is biaxial positive, $2V_{est.} = 85\pm4°$, $2V_{calc.} = 88°$, $r > v$ weak. Pleochroism is medium-strong: $X$ pale reddish brown, $Y$ yellowish brown, $Z$ dark yellowish brown; absorption $Z > Y > X$. The orientation is $X = b$, $Y \approx a$, $Z \approx c$, and the elongate fragments of the mineral always show positive optical elongation. Small grains show slightly anomalous bluish grey interference colours. Platy grains show no obvious zonal growth and no variation of the refractive indices, thus indicating chemical homogeneity of the grains. No twin lamellae or other indications of twinning were observed. In contrast, whitmoreite, the phosphate analogue of bendadaite, is invariably twinned parallel to {100} (Moore *et al.*, 1974). No fluorescence was observed in either short- or long-wave ultraviolet light.

The optical properties of the co-type material (Brazil) were determined on two different materials. Dark brown bunches of fibres or divergent plates have $\alpha$ 1.720(4), $\beta$ 1.760(4), $\gamma$ 1.787(4), with $2V \approx 90°$, $Z \wedge c \approx 10-20°$, and
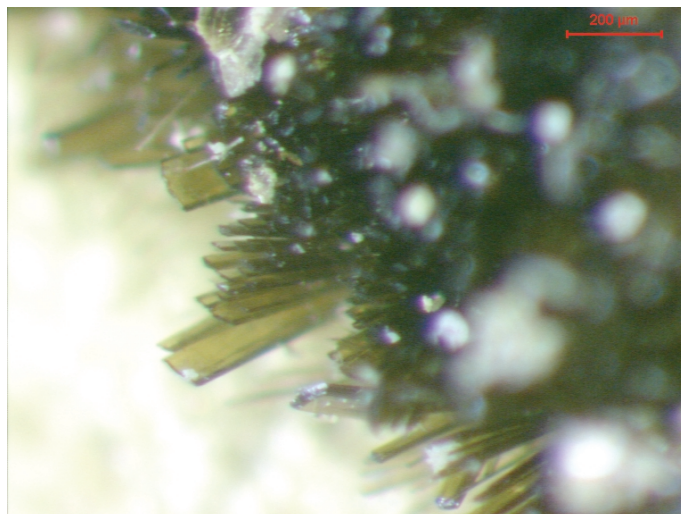


FIG. 3. Tabular crystals of co-type bendadaite. The appearance of these crystals is similar to those of cobaltarthurite, *cf.* Jambor *et al.* (2002).

medium-strong pleochroism, $Z$ (dark brown) > $X$, $Y$ (greenish brown). Bunches of very fine divergent colourless to pale yellow needles (1−3 µm) are characterized by $\alpha$ 1.725(5), $\beta$ 1.755(5), $\gamma$ 1.785(5), $2V \approx 90$, $Z \wedge c \approx$ 10−12º, and recognizable pleochroism, $Z > Y = X$.

The pleochroic colour scheme of the co-type material (dark brown, greenish brown) suggests that the Brazilian material has a slightly greater $Fe^{2+}/Fe^{3+}$ ratio than the type material (no greenish hues, indicating more oxidized Fe), see also discussion further below.

## Chemical composition

Preliminary, semi-quantitative, energy-dispersive analyses of type bendadaite were conducted with a Cambridge scanning electron microscope (CamScan 44, EDAX PV9900). The analyses showed the mineral to contain major Fe and As, minor P, and very small amounts of Zn and Mn. No other elements with atomic number >10 were detected. The approximate ratio (Fe + Mn + Zn)/(As + P) was ~1.54. The As/P ratio in crystal aggregates with different appearances showed only a small variability. From one EDS analysis of the type specimen, the approximate, idealized formula $(Fe^{2+}_{0.90}Mn_{<0.01}Zn_{<0.01})Fe^{3+}_2[(As_{0.91}P_{0.09})O_4]_2(OH)_2 \cdot 4H_2O$ was derived. Very similar results were also obtained from semi-quantitative analyses using a Cambridge Stereoscan 200 (Link AN 10000 detector). During the SEM-EDS analyses the crystal aggregates partly dehydrated and developed cracks approximately perpendicular to their elongation (Fig. 2). Subsequent semi-quantitative EDS analyses conducted in a TEM at 200 kV confirmed the minor variability of the As:P ratio. Other impurity elements (except P) detected were Ca, Zn, Mn, Al and S, all in very minor to trace amounts. A visible, albeit small, variation was especially found for the Ca content.

A Cameca electron microprobe (Camebax SX51) was used to determine the accurate chemical composition of type bendadaite. Experimental conditions were: acceleration voltage 15 kV, beam current 20 nA, count time 20 s, fully focused beam. The following standards were used: $Fe_2O_3$ (Fe), $Al_2O_3$ (Al), rhodonite (Mn), ZnS (Zn), wollastonite (Ca), periclase (Mg), K-feldspar (K), Cu metal (Cu), $SnO_2$ (Sn), GaAs (As), syn. hydroxylapatite (P) and marcasite (S). Elements present as negligible traces or undetectable were K, Ba and Cl.

Wavelength-dispersive scans did not reveal additional components. The electron microprobe analyses yielded (wt.%): CaO 0.04, MnO 0.03, CuO 0.06, ZnO 0.04, $Fe_2O_3$ (total) 43.92, $Al_2O_3$ 1.15, $SnO_2$ 0.10, $As_2O_5$ 43.27, $P_2O_5$ 1.86, $SO_3$ 0.03. The empirical formula is $(Fe^{2+}_{0.52}Fe^{3+}_{0.32}\square_{0.16})_{\Sigma 1.00}(Fe^{3+}_{1.89}Al_{0.11})_{\Sigma 2.00}(As_{1.87}P_{0.13})_{\Sigma 2.00}O_8(OH)_{2.00} \cdot 4H_2O$, based on 2(As, P) and assuming ideal 8O, 2(OH), $4H_2O$ and complete occupancy of the ferric iron site by $Fe^{3+}$ and Al. The majority of the excess iron was assumed to be divalent because microchemical tests for ferrous iron (using Merckoquant 10.004, Merck, Germany) were positive. The water content could not be determined directly due to the very small quantity of material. The analytical data are compared with theoretical values in Table 1. The wt.% values obtained are somewhat larger than the theoretical values, and indicate that the fully focused beam caused some dehydration of the sample (as observed in the prior SEM-EDS studies), also consistent with the observation that the beam produced a tiny hole in the polished surface. Thermal studies (see below) suggest that water loss starts at >150º, a temperature certainly induced by a fully focused beam. A complete loss of the four $H_2O$ molecules present in the structure probably occurs at >250º (see below) and would theoretically result in a measurable (Fe+As) total of 65.38 element wt.%. The calculated atomic ratios (Fe+Al+Ca+Mn+Zn+Cu+Sn)/(As+P+S) vary between 1.38 and 1.48 (average 1.43; ideally: 1.5) and indicate the presence of some vacancies on the Fe(1) site (for further discussion see below). The empirical formula corresponds to an 84% occupancy of the Fe(1) site; if the very minor amounts of Ca, Mn, Cu, Zn and Sn are also taken into account, the occupancy would be close to 86%.

The results of electron microprobe analyses of co-type bendadaite are given in Table 1 (standards used: $Fe_2O_3$ for Fe, Mn metal for Mn, $Al_2O_3$ for Al, As metal for As, $LaPO_4$ for P; $H_2O$ determined by the Alimarin method, a modification of the Penfield method; the division of iron between $Fe^{2+}$ and $Fe^{3+}$ was made on the basis of Mössbauer spectroscopy data). The analytical total is again somewhat high, and attributed to dehydration of the sample under the beam. The empirical formula derived, $(Fe^{2+}_{0.69}Fe^{3+}_{0.13}Mn_{0.04}\square_{0.14})_{\Sigma 1.00}(Fe^{3+}_{1.93}Al_{0.07})_{\Sigma 2.00}(As_{1.62}P_{0.38})_{\Sigma 2.00}O_8(OH)_{1.82} \cdot 4.18H_2O$, is slightly Al- and P-richer than that of the type material. The vacancy in the

TABLE 1. Chemical composition of bendadaite (wt.%).

| | 1 | 1 (range) | 2 | 2 (range) | 3 |
|---|---|---|---|---|---|
| CaO | 0.04 | 0.01−0.06 | | | |
| MnO | 0.03 | 0.00−0.06 | 0.57 | 0.00−1.77 | |
| CuO | 0.06 | 0.00−0.21 | | | |
| ZnO | 0.04 | 0.00−0.11 | | | |
| FeO | | | 10.07[1] | | 13.03 |
| $Fe_2O_3$ | | | 33.22[1] | | 28.96 |
| $Fe_2O_3$* | (43.92) | (42.69−44.51) | (44.40) | (43.65−45.22) | |
| $Al_2O_3$ | 1.15 | 0.83−1.28 | 0.72 | 0.00−1.12 | |
| $SnO_2$ | 0.10 | 0.04−0.19 | | | |
| $As_2O_5$ | 43.27 | 42.38−44.79 | 37.72 | 36.32−39.61 | 41.68 |
| $P_2O_5$ | 1.86 | 1.51−2.18 | 5.40 | 3.71−6.92 | |
| $SO_3$ | 0.03 | 0.00−0.10 | | | |
| $H_2O$ | n.a. | | 18.60[2] | 18.49−18.71 | 16.33 |
| Total | | | 106.30 | | 100.00 |

* All Fe as $Fe^{3+}$
(1) Bendada, Portugal; nine spot analyses; analyst − U.K.; n.a. = not analysed.
(2) Lavra do Almerindo, Linópolis, Divino das Laranjeiras county, Minas Gerais, Brazil; analyst − N.C.; five spot analyses on dark material (see text).
(3) Ideal bendadaite, $Fe^{2+}Fe_2^{3+}(AsO_4)_2(OH)_2 \cdot 4H_2O$.
[1] from Mössbauer data on pale crystals; see text.
[2] by the Alimarin method.

formula is consistent with the results of the crystal-structure refinement.

## Infrared, Raman and Mössbauer spectroscopy

Direct evidence for the presence of molecular water, hydroxyl and arsenate groups was obtained by micro-infrared (IR) spectroscopy of a single cleavage flake of type bendadaite. The spectrum shows arsenate bands, a sharp peak at 1651 cm$^{-1}$ ($H_2O$ bending vibration), and a broad band at 3000−3500 cm$^{-1}$ (OH groups). The latter band was somewhat affected by absorption due to the cleavage thickness being too large. The IR spectrum of cobaltarthurite (Jambor et al., 2002) is similar.

Single-crystal Raman spectroscopy was used to confirm the presence of OH in type bendadaite. The spectrum was obtained with a dispersive Jobin Yvon T 64.000 triple monochromator system equipped with a Olympus BX40 microscope, using 676 nm Kr$^+$ excitation. The spectrum shows two distinct bands in the OH-stretching region, the relatively low frequencies (3385 and 3275 cm$^{-1}$) of which point to medium-weak hydrogen bonds, with O···O distances of ~2.80

and 2.75 Å. Internal stretching vibrations of the $AsO_4$ groups (multiplet at ~800 cm$^{-1}$) as well as lattice modes and vibrations involving $Fe^{2+}$ and $Fe^{3+}$ ions are sharp and intense. The two OH bands are superposed on an intense broad background or broad band. Although this could hypothetically be due to molecular water, the intensity of the broad band seems to be a bit too high to be unambiguously interpreted as a $H_2O$ band. In the H−O−H bending region, there is a very weak band at 1690 cm$^{-1}$, indicating strong hydrogen bonding. The assignment of this band to $H_2O$ would be consistent with the position of the broad "band" in the stretching region. The complex appearance of the <1200 cm$^{-1}$ spectrum is in agreement with the low symmetry of the mineral and the presence of two different Fe sites in the structure. Note that Raman spectra reported for arthurite and whitmoreite by Frost et al. (2003) are considered unreliable because these authors suggest the presence of distinct carbonate in both minerals.

A specimen of co-type bendadaite (dark brown variety) was mixed with anhydrous KBr, pelletized, and analysed using a Specord 75 IR spectrophotometer (Fig. 4). The IR spectrum of
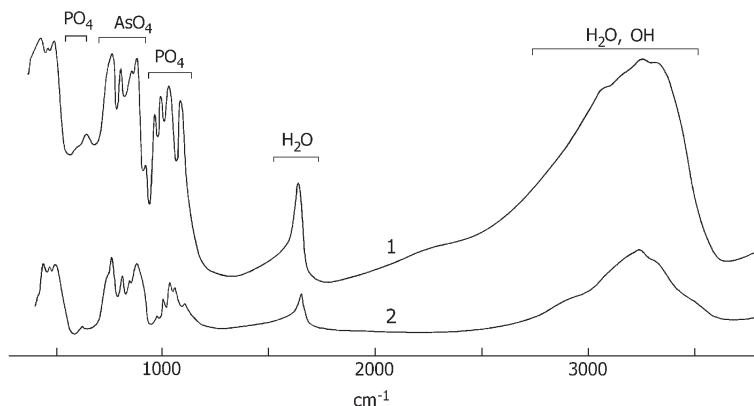
FIG. 4. IR spectra of co-type bendadaite (dark brown variety) (1) and arthurite (2).

a pure KBr disk was subtracted from the overall spectrum. Polystyrene and gaseous $NH_3$ were used as frequency standards; the precision of frequency measurement was $\pm 1$ cm$^{-1}$; the mean resolution for the region $400-1600$ cm$^{-1}$ was $0.8$ cm$^{-1}$. Wavenumbers of absorption bands (cm$^{-1}$) and their assignments are (s − strong bands, sh − shoulder): 3220s, 3250s, 3085sh (O−H stretching vibrations), 1643 (bending vibrations of $H_2O$ molecules), 1092, 1045sh, 1033s, 995, 969 (stretching vibrations of $PO_4^{3-}$ groups), 925, 881s, 854s, 811s, 768s (stretching vibrations of $AsO_4^{3-}$ groups), 650, 620sh (bending vibrations of $PO_4^{3-}$ groups), 490s, 467s, 431s (mixed modes involving O−As−O angles and

Fe−O bonds). The IR spectrum of bendadaite is similar to spectra of other arsenate members of the arthurite group.

A Mössbauer spectrum of pale crystals from the co-type material (Fig. 5) was obtained using a Wissel device at 293 K, with accumulation of the signal in 512 channels during 51.8 h. Two symmetric doublets are observed. The doublet with an isomer shift of 0.2635 mm/s, quadrupole splitting of 0.466 mm/s and relative area of 74.8% corresponds to $Fe^{3+}$. The doublet with an isomer shift of 1.250 mm/s, quadrupole splitting of 2.038 mm/s and relative area of 25.2% corresponds to $Fe^{2+}$. The derived atomic ratio $Fe^{3+}:(Fe^{2+} + Fe^{3+})$ is equal to 0.748(12),
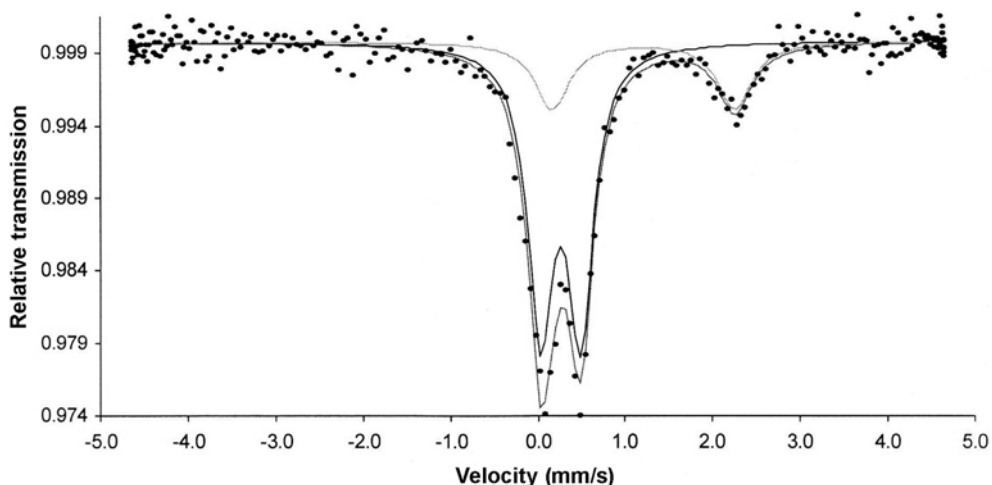


FIG. 5. Mössbauer spectrum of co-type bendadaite (pale variety).

TABLE 2. X-ray powder diffraction data for bendadaite, compared with data for ojuelaite.

| | Bendadaite (this work, type material)[1] | | | | Bendadaite (this work, co-type material; dark crystals) | | Ojuelaite (Cesbron *et al.*, 1981; Hughes *et al.*, 1996) | | |
| --- | --- | --- | --- | --- | --- | --- | --- | --- | --- |
| $I_{meas}$ | $I_{calc}$[2] | $d_{meas.}$ | $d_{calc.}$ | hkl | $I_{meas.}$ | $d_{meas.}$ | $I_{calc.}$[3] | $d_{calc.}$ | hkl |
| **10** | **10.0** | **10.22** | **10.21** | **100** | **10.0** | **10.18** | 9.6 | 10.21 | 100 |
| **8** | **9.1** | **7.036** | **7.038** | **110** | **9.1** | **7.02** | 10.0 | 7.02 | 110 |
| 1 | 1.0 | 5.094 | 5.106 | 200 | 0.7 | 5.081 | 0.8 | 5.11 | 200 |
| 3b | 3.5, | 4.833 | 4.857, | 020, | 0.8 | 4.857 | 4.8 | 4.83, | 020, |
| | 2.3 | | 4.811 | 011 | | | 3.5 | 4.82 | 011 |
| 2 | 2.0 | 4.520 | 4.520 | 210 | 1.0 | 4.513 | 2.3 | 4.516 | 210 |
| 0.5 | 0.6 | 4.381 | 4.386 | 120 | 0.6 | 4.375 | 0.8 | 4.369 | 120 |
| **5** | **6.8** | **4.250** | **4.251** | **111** | **1.5** | **4.245** | 9.5 | 4.249 | 111 |
| – | 0.1 | – | 3.651 | 021 | – | – | 0.1 | 3.645 | 021 |
| – | 0.6 | – | 3.519 | 220 | 0.6 | 3.509 | 0.5 | 3.510 | 220 |
| 2b | 2.1 | 3.490 | 3.491 | $\bar{1}21$ | – | – | 2.1 | 3.489 | $12\bar{1}$ |
| 1 | 0.6, | 3.403 | 3.404, | 300, | 0.5 | 3.391 | 1.0 | 3.406, | 300, |
| | 0.6 | | 3.398 | 211 | | | 0.5 | 3.394 | 211 |
| 1 | 1.2 | 3.085 | 3.086 | 130 | **1.5** | **3.086** | 1.5 | 3.072 | 130 |
| 2 | 2.6 | 3.037 | 3.039 | $\bar{2}21$ | – | – | 2.9 | 3.040 | $22\bar{1}$ |
| 3 | 4.2 | 2.907 | 2.906 | 221 | – | – | 4.1 | 2.900 | 221 |
| **4** | **6.3** | **2.865** | **2.864** | **$\bar{3}11$** | **1.5** | **2.896** | 7.7 | 2.871 | $31\bar{1}$ |
| 1b | 0.8, | 2.790 | 2.795, | 031, | – | – | 1.0, | 2.787, | 031, |
| | 1.0 | | 2.788 | 320 | | | 1.5 | 2.784 | 320 |
| 2 | 2.0 | 2.729 | 2.734 | 230 | 1.3 | 2.730 | 2.1 | 2.725 | 230 |
| 0.5 | 0.4, | 2.671 | 2.671 | 131, | – | – | 0.5, | 2.669, | 012, |
| | 0.5 | | | 012 | | | 0.6 | 2.663 | 131 |
| 2 | 1.2, | 2.624 | 2.625, | 102, | – | – | 1.7 | 2.629, | 102, |
| | 1.9 | | 2.621 | $\bar{1}12$ | | | 1.9 | 2.629 | $11\bar{2}$ |
| 0.5 | 0.2, | 2.543 | 2.553, | 400, | – | – | 0.4, | 2.554, | 400, |
| | 0.1, | | 2.551, | $\bar{3}21$, | | | 0.1 | 2.553 | $32\bar{1}$ |
| | 0.1 | | 2.534 | 112 | | | | | |
| 0.5 | 1.1 | 2.511 | 2.511 | $\bar{2}02$ | – | – | 1.6 | 2.522 | $20\bar{2}$ |
| – | 0.2 | – | 2.534 | $\bar{2}31$ | – | – | 0.3 | 2.487 | $23\bar{1}$ |
| – | 0.3 | – | 2.469 | 410 | – | – | 0.3 | 2.469 | 410 |
| 1 | 1.6 | 2.434 | 2.433 | 321 | – | – | 0.04, | 2.439, | $21\bar{2}$, |
| | | | | | | | 1.9 | 2.429 | 321 |
| 0.5 | 0.5 | 2.364 | 2.363 | 140 | – | – | 0.7 | 2.351 | 140 |
| 1b | 0.5 | 2.297 | 2.297 | 212 | – | – | 0.7 | 2.297 | 212 |
| – | 0.1 | – | 2.260 | 420 | – | – | 0.04 | 2.258 | 420 |
| 2b | 0.2, | 2.225 | 2.228, | $\bar{3}02$, | – | – | 1.9 | 2.215 | 041 |
| | 1.7 | | 2.224 | 041 | | | | | |
| 2b | 1.0 | 2.196 | 2.199 | 411 | – | – | 1.8 | 2.197 | 411 |
| 0.5 | 0.3 | 2.158 | 2.160 | 141 | – | – | 0.4 | 2.152 | 141 |
| – | 0.2 | – | 2.140 | $\bar{4}21$ | – | – | 0.3 | 2.143 | $42\bar{1}$ |
| 1b | 1.0, | 2.129 | 2.126, | 222, | – | – | 1.0, | 2.124, | 222, |
| | 0.5 | | 2.123 | 331 | 0.6 | 2.116 | 0.7 | 2.118 | 331 |
| 0.5 | 0.7 | 2.105 | 2.104 | 032 | – | – | 1.0 | 2.103 | 032 |
| 0.5 | 0.5 | 2.086 | 2.084 | $\bar{1}32$ | – | – | 0.7 | 2.084 | $13\bar{2}$ |
| 1b | 0.3, | 2.051 | 2.061, | $\bar{2}41$, | – | – | 0.9, | 2.045, | 421, |
| | 0.9, | | 2.047, | 421, | | | 0.2 | 2.043 | 500 |
| | 0.2 | | 2.043 | 500 | | | | | |
| 1b | 0.9 | 2.024 | 2.025 | $\bar{3}22$ | – | – | 1.0, | 2.030, | $32\bar{2}$, |
| | | | | | | | 0.001 | 2.029 | 312 |
| – | 0.2 | – | 1.999 | 510 | – | – | 0.3 | 1.999 | 510 |
| – | 0.5 | – | 1.977 | 340 | – | – | 0.6 | 1.970 | 340 |

Table 2 (*contd.*)

| | Bendadaite (this work, type material)[1] | | | | Bendadaite (this work, co-type material; dark crystals) | | Ojuelaite (Cesbron *et al.*, 1981; Hughes *et al.*, 1996) | | |
|---|---|---|---|---|---|---|---|---|---|
| $I_{meas}$ | $I_{calc}$[2] | $d_{meas.}$ | $d_{calc.}$ | *hkl* | $I_{meas.}$ | $d_{meas.}$ | $I_{calc.}$[3] | $d_{calc.}$ | *hkl* |
| 1b | 0.5, 0.1, 0.3 | 1.912 | 1.920, 1.909, 1.908 | $\bar{4}$31, 232, 150 | – | – | 0.5, 0.8 | 1.920, 1.900 | 43$\bar{1}$, 150 |
| 1b | 0.3, 0.5 | 1.820 | 1.826, 1.820 | 042, $\bar{5}$21 | – | – | 0.3, 0.4, 0.6 | 1.832, 1.823, 1.821 | 341, 042, 52$\bar{1}$ |
| 1b | 0.9 | 1.749 | 1.748 | $\bar{2}$13 | – | – | – | – | – |
| 1b | 0.1, 0.5 | 1.715 | 1.720, 1.713 | $\bar{1}$23, 251 | – | – | – | – | – |
| 1b | 0.4, 0.6 | 1.698 | 1.699, 1.694 | 422, 242 | – | – | – | – | – |
| 1b | 0.4, 0.2, 0.8 | 1.677 | 1.678, 1.677, 1.672 | $\bar{5}$12, 610, 213 | – 0.8 – | – 1.685 – | – | – | – |
| 0.5b | 0.2 | 1.654 | 1.649 | $\bar{3}$13 | – | – | – | – | – |
| 1b | 0.3, 0.1 | 1.635 | 1.637, 1.630 | $\bar{6}$11, $\bar{3}$51 | – | – | – | – | – |
| 1b | 0.1, 0.1 | 1.603 | 1.607, 1.606 | $\bar{5}$22, 620 | – | – | – | – | – |
| 0.5 | 0.2, 0.3 | 1.560 | 1.563, 1.562 | 540, 152 | – | – | – | – | – |
| 1 | 0.5, 0.5 | 1.543 | 1.546, 1.543 | 450, 260 | – | – | – | – | – |
| 0.5 | 0.1 | 1.526 | 1.526 | $\bar{5}$41 | – | – | – | – | – |
| 2 | 0.2, 0.3, 0.5, 0.4, 0.1, 0.6 | 1.504 | 1.507, 1.507, 1.506, 1.501, 1.499, 1.499 | $\bar{5}$32, 630, $\bar{4}$51, 252, 323, $\bar{6}$02 | – | – | – | – | – |

[1] 114.6 mm Debye-Scherrer camera, filtered Fe-$K\alpha$ radiation ($\lambda = 1.9373$ Å); sample diameter 0.15 mm, visually estimated intensities; *d* spacings in Å; b = broad. Refined unit-cell parameters: $a = 10.239(3)$ Å, $b = 9.713(2)$ Å, $c = 5.552(2)$ Å, $\beta = 94.11(2)°$, $V = 550.7(2)$ Å$^3$, space group $P2_1/c$, Z = 2.
[2] Theoretical intensities for bendadaite were calculated using the structure model obtained from the Brazilian co-type material (program Lazy Pulverix; Yvon *et al.*, 1977).
[3] Theoretical intensities for ojuelaite were calculated using the atomic coordinates given for ojuelaite (Hughes *et al.*, 1996). A number of *hkl* data with measurable calculated intensities had to be added to the *hkl*-list reported by Cesbron *et al.* (1981).
Strongest lines in bold

supporting a small replacement of $Fe^{2+}$ by $Fe^{3+}$ as the ideal formula would have $Fe^{3+}:(Fe^{2+} + Fe^{3+}) = 0.67$.

## Thermal studies

Due to the very small amount of type material, no thermoanalytical studies could be performed. Therefore, heating experiments were conducted on tiny, pure fragments of bendadaite. The fragments were heated in air in a Pt crucible at 100ºC for 2 h, then at 200, 300, 400 and finally at 700ºC (each for 2 h). After each heating period, the powder pattern of one of the uncrushed fragments was investigated using a 57.3 mm Gandolfi camera and Cr-$K\alpha$ radiation.

After heating at 100ºC, the fragments' appearance (colour, lustre and transparency) and powder

pattern were unchanged. Heating at 200ºC induced a slightly lowered transparency and lustre (presumably due to loss of some loosely bound water), but again no change in the powder pattern. Heating at 300ºC changed the colour to brown (with a reddish tinge) and the fragments had lost most of their transparency; the lustre on the cleavage faces appeared more pearly; the powder pattern had changed completely and now showed strong lines at 2.76 and 2.47 Å; the complete pattern is [$d(I)$]: 3.79(0.5), 3.64(2), 3.42(3), 2.95(1), 2.76(10), 2.68(2b), 2.47(9), 2.20(2b), 2.09(0.5), 1.871(0.5), 1.725(1b), 1.613(0.5b), 1.522(3b), 1.443(1.5), 1.423(0.5) and 1.497(1.5) Å. The colour change and the unknown structural change were probably caused by a combination of loss of water and an oxidation of $Fe^{2+}$ to $Fe^{3+}$. Heating at 400ºC caused the complete loss of transparency and an increased pearly lustre; the powder pattern was very similar, albeit not completely identical to that of the fragment heated at 300ºC. After the final heating step at 700ºC, the heating product appeared reddish brown to dark brown; the powder pattern, comprising 24 lines, had strong reflections at 3.50($I$ = 10), 1.445(3b), 4.42(2), 2.40(2), 2.21(2), 1.907(2) and 1.605(2b) Å. These strongest reflections, except for 2.21(2), are similar to those of synthetic, quartz-type $FeHAsO_4$ (ICDD-PDF 22-340) prepared from heating non-stoichiometric scorodite at 530−570ºC. The remaining ~20 reflections could not be attributed to a known compound.

Bendadaite therefore shows a thermal behaviour similar to that of ojuelaite, its Zn analogue. Ojuelaite loses water at ~198 and ~250ºC and recrystallizes at ~607ºC according to the DTA/TG studies of Cesbron *et al.* (1981); fusion and loss of $As_2O_3$ occur at ~984 and ~1057ºC (heating rates: DTA 600ºC/h, TG 300ºC/h).

A thermogravimetric study of co-type material could not be conducted. Chemical analysis of the dark crystals gave $H_2O$ contents of 18.49−18.71 wt.%, reasonably close to expected values (ideal, Al- and P-free bendadaite has 16.33 wt.%, Table 1).

### X-ray diffraction and crystal structure

Indexed X-ray powder diffraction data of type bendadaite were obtained with a 114.6 mm diameter Debye-Scherrer camera and filtered Fe-$K\alpha$ radiation ($\lambda$ = 1.9373 Å), and are listed in Table 2. The powder data clearly demonstrate that bendadaite belongs to the arthurite group, which comprises the arsenates arthurite (Davis and Hey, 1964 and 1969; Walenta, 1975; Keller and Hess, 1978), ojuelaite (Cesbron *et al.*, 1981; Hughes *et al.*, 1996) and cobaltarthurite (Jambor *et al.*, 2002; Raudsepp and Pani, 2002; see also Kampf *et al.*, 2004 and Kampf, 2005), and the phosphates whitmoreite (Moore *et al.*, 1974), earlshannonite (Peacor *et al.*, 1984) and kunatite (Mills *et al.*, 2008).

Further unnamed Zn-$Fe^{3+}$ and $Fe^{2+}$-Al phosphate members of the arthurite group were also reported by Sejkora *et al.* (2006) from Krásno, Czech Republic. The latter phase ("UNK8"; Sejkora *et al.* 2006) forms as tiny zones (up to 40 μm) within kunatite crystals (the presence of divalent iron in this phase is deduced from stoichiometry). A possible $Mn^{2+}$-$Mn^{3+}$-As member from Falotta, Switzerland, which forms small red crystals, is mentioned on http://home-page.swissonline.ch/KlingerMinerals/mineralien-falotta-e.htm.

The general formula of these minerals is $X^{2+}Y_2^{3+}(ZO_4)_2(OH)_2 \cdot 4H_2O$, where $X$ is Fe, Mn, Cu or Zn, $Y$ is Fe, Al, and presumably Mn, and $Z$ is P or As, with minor S. Table 2 shows that the $d$ spacings of bendadaite are very similar to those of the Zn-$Fe^{3+}$-arsenate end-member ojuelaite (Cesbron *et al.*, 1981; Hughes *et al.*, 1996). The powder data for bendadaite were easy to index according to the space group $P2_1/c$, typical of the arthurite-group members. The indexing is based on a theoretical powder pattern calculated using the positional parameters of ojuelaite (Hughes *et al.*, 1996). A comparison between the measured and calculated intensities is made within the discussion of the probable occurrence of vacancies in the structure of bendadaite (see below). The refined unit-cell parameters are: $a$ = 10.239(3), $b$ = 9.713(2), $c$ = 5.552(2) Å, $\beta$ = 94.11(2)º, $V$ = 550.7(2) Å$^3$, and Z = 2. They are fairly close to the values reported for ojuelaite ($a$ = 10.247(6) / 10.237(1), $b$ = 9.665(5) / 9.662(3), $c$ = 5.569(4) / 5.562(1) Å, $\beta$ = 94.36 [no s.u. given] / 94.36(1)º, $V$ = 549.4 / 548.5 Å$^3$; values given by Cesbron *et al.*, 1981 and Hughes *et al.*, 1996, respectively). This is not surprising, as the radius of $^{[6]}Fe^{2+}$, 0.78 Å, is very similar to that of $^{[6]}Zn^{2+}$, 0.74 Å (Shannon, 1976), resulting in similar-sized unit cells. Bendadaite can be differentiated from the other members of the arthurite group by chemical analysis and X-ray investigations; Table 3 provides a detailed comparison with the arsenate members.

TABLE 3. Comparison of data from ojuelaite, arthurite, cobaltarthurite and bendadaite.

| Formula | Ojuelaite[1] $Zn^{2+}Fe_2^{3+}(AsO_4)_2(OH)_2\cdot4H_2O$ | Arthurite[2,3,4,5] $Cu^{2+}Fe_2^{3+}(AsO_4)_2(OH)_2\cdot4H_2O$ | Cobaltarthurite[6] $Co^{2+}Fe_2^{3+}(AsO_4)_2(OH)_2\cdot4H_2O$ | Bendadaite[7] $(Fe^{2+},Fe^{3+},\square)Fe_2^{3+}$ $(AsO_4)_2(OH)_2\cdot4H_2O$ |
|---|---|---|---|---|
| $a$ (Å) | 10.247(6) | 10.189(2)[2] | 10.2694(4) | 10.239(3) |
| $b$ (Å) | 9.665(5) | 9.649(2)[2] | 9.6790(3) | 9.713(2) |
| $c$ (Å) | 5.569(4) | 5.598(1)[2] | 5.5723(2) | 5.552(2) |
| $\beta$ (°) | 94.36 | 92.16(2)[2] | 94.277(2) | 94.11(2) |
| $V$ (Å³) | 549.37 | 549.9(2)[2] | 552.33(3) | 550.7(2) |
| Five strongest lines in the powder pattern, $d$ in Å ($I$ in %) | 4.251(100), 2.871(90), 7.03(82), 4.83(78), 10.23(65) | 6.98(100), 10.14(75), 4.812(60), 2.812(50), 4.305(45)[5] | 10.2(95), 7.04(100), 4.81(65), 4.24(60), 2.89(25) | 10.22(100), 7.036 (80), 4.250(50), 2.865(40), 4.833(30) |
| $D_{meas.}$, $D_{calc.}$ | 3.39, 3.39 | ~3.2, 3.29[3] | 3.22(2), 3.179–3.248 | 3.15(10), 3.16 |
| Mohs hardness | 3 | not given | 3.5–4 | ~3 |
| $\alpha$ | 1.696 | 1.746(3)[2] | 1.741 | 1.734(3) |
| $\beta$ | 1.730 | 1.774(3)[2] | 1.762 | 1.759(3) |
| $\gamma$ | 1.798 | 1.806(3)[2] | 1.797 | 1.787(4) |
| Optic sign | pos. | pos. | pos. | pos. |
| $2V_{meas.}$, $2V_{calc.}$ | not meas., 73° | not meas.[2], 88°[2]; near 90°[4], 88.6[4] | not meas., 77° | 85(4)°, 88° |
| Dispersion | not given | not given | not given | $r>v$ weak |
| OAP | not given | (010)[4] | not given | (010) |
| Orientation | $X = b$, $Z = c$ | $Y = b$, $Z\wedge c = 10$°[4] | probably $Z = c$ | $X = b$, $Y \sim a$, $Z \sim c$ |
| $X$ (colour) | 'pleochroic in yellow' | pale yellow[2] colourless to pale green[4] | colourless | pale reddish brown |
| $Y$ (colour) | | yellow-green[2] grass green[4] | not given | yellowish brown |
| $Z$ (colour) | | yellow-green[2] grassy olive-green[4] | medium yellow | dark yellowish brown |
| Absorption | $Z = X > Y$ | $Z > Y > X$ | $Z > X$, $Y$ | $Z > Y > X$ |
| Twinning | not given | not given | not given | none observed |
| Cleavage | (010) good | not given | none observed | (010) good |

[1] Cesbron *et al.* (1981) [no s.u. given for β]; [2] Keller (1978); [3] Davis and Hey (1969), contains P and S (see also Davis and Hey, 1964; Clark and Sillitoe, 1969); [4] Walenta (1975); [5] ICDD-PDF 36-400, contains minor Si, P; [6] Jambor *et al.* (2002) and Raudsepp and Pani (2002) (contains some Mg, Fe³⁺, Mn and P); see also Kampf *et al.* (2004) and Kampf (2005); [7] this work (type material).

Attempts to separate single cleavage fragments from the radiating aggregates of bendadaite from the type locality were unsuccessful. However, after some effort, a tiny, elongate cleavage fragment composed of several subparallel, flattened crystals suitable for X-ray film investigations was isolated. It was mounted on a glass fibre, with its axis parallel to the elongation of the glass fibre, and investigated by a 60 mm diameter rotation camera (using filtered Co-$K\alpha$ radiation). The intensities and indices of reflections on the observed zero, $1^{st}$ and $2^{nd}$ layers were in agreement with expected values and the X-ray powder diffraction data. The spacing between the layers on the rotation film corresponds to an approximate $d$ spacing of ~5.52 Å, in fairly good agreement with the refined value for the unit-cell parameter $c$, 5.552(2) Å. Additional Weissenberg and precession photographs provided further evidence of an arthurite-type structure. All spots on the precession films were imperfect and indicated the presence of at least four subparallel individuals. The approximate monoclinic angle $\beta$ derived from the $h0l$ pattern, ~93.8°, is in good agreement with the refined value of 94.11(2)°. Both films clearly showed the extinctions due to the $c$ glide plane; the $0kl$ pattern additionally showed the extinctions due to the $2_1$ screw axis. Precession photography proved that the cleavage plane is parallel to {010}, *i.e.* identical to that of its Zn analogue ojuelaite.

The crystallography of bendadaite from the type material was also studied in detail by TEM. Gently crushed fragments of the mineral were deposited from an acetone suspension onto Cu grids with holey carbon supporting films. The fragments were examined at 200 kV in a Philips CM 200 TEM fitted with a double tilt goniometer at the Centre for Electron Microscopy and Microstructural Analysis, Adelaide, Australia (now Adelaide Microscopy). The mineral was stable under the chosen conditions and good selected area electron diffraction (SAED) patterns could be obtained. Due to the pronounced cleavage parallel to {010}, most of the bendadaite fragments were lying with {010} parallel to the grid surface; thus, the unit-cell parameter $b$ could only be measured from a single fragment. The SAED patterns obtained confirm the monoclinic symmetry and the proposed unit cell, and the measured unit-cell parameters are in reasonably good agreement with the values obtained from the refinement of the X-ray powder data [$a = 10.239(3)$, $b = 9.713(2)$, $c = 5.552(2)$ Å, $\beta = 94.11(2)°$]. The quality of the crystal fragments did not allow the observation of

the extinctions caused by the $2_1$ screw axis and the $c$ glide plane. In general, the effect of multiple diffraction in TEM work commonly precludes the observation of extinctions caused by glide planes and screw axes; these extinctions are only observable if perfect, homogeneous crystals are investigated and specialized alignment techniques are used in combination with convergent beam diffraction studies. Over-exposed SAED patterns provided no evidence for a superstructure in bendadaite.

A single-crystal structure determination was feasible using a crystal from the co-type material. This crystal was measured with a Bruker AXS KAPPA APEX II diffractometer equipped with a CCD area detector (see Table 4). The structure was solved (in space group $P2_1/c$) and refined using SHELXS-97 and SHELXL-97 (Sheldrick, 2008), respectively. The final steps of refinement, using the non-H coordinate set of whitmoreite (Moore *et al.*, 1974) and the H atom coordinates of cobaltarthurite as a starting model gave $R(F) = 1.6\%$. All hydrogen atoms (both from $H_2O$ and OH) were found and freely refined. The structure model is in good agreement with those of the other arsenate members of the arthurite group and resulted in the formula $(Fe^{2+}_{0.95}\square_{0.05})_{\Sigma 1.00}$ $(Fe^{3+}_{1.80}Al_{0.20})_{\Sigma 2.00}(As_{1.48}P_{0.52})_{\Sigma 2.00}O_8$ $(OH)_2 \cdot 4H_2O$ (minor Mn neglected); the positions of the hydrogen atoms are equivalent to those in cobaltarthurite (Kampf, 2005) and the site designations of the latter were accordingly adopted. If occupancy of the $Fe^{2+}$ is refined, a value of 95% is obtained. This deficit appears to be real, since a similar deficit was also observed in the structure of whitmoreite (Moore *et al.*, 1974), as discussed below. The hydrogen-bonding scheme is characterized by O···O donor-acceptor distances in very good agreement with those derived from the IR-spectroscopic data.

The refined positional and displacement parameters are given in Tables 5 and 6, and selected bond lengths in Table 7. A list of observed and calculated structure factors has been deposited at http://www.minersoc.org/pages/e_journals/ dep_mat_mm.html. A view of the overall connectivity is given in Fig. 6; for details the reader is referred to previous reports discussing the crystal structure of arthurite-type minerals.

Bond-valence calculations (parameters from Brese and O'Keeffe, 1991) gave 2.10 valence units (v.u.) for the $Fe^{2+}$ site (Mn ignored) and 2.95 v.u. for the $Fe^{3+}$ site (Al ignored). The refined single-crystal cell parameters of the co-

TABLE 4. Crystal data, data collection and refinement details for bendadaite from co-type locality.

**Crystal data**

| | |
|---|---|
| Formula | $(Fe^{2+}_{0.95}\square_{0.05})_{\Sigma1.00}(Fe^{3+}_{1.80}Al_{0.20})_{\Sigma2.00}(As_{1.48}P_{0.52})_{\Sigma2.00}O_8(OH)_2\cdot4H_2O$ |
| Space group | $P2_1/c$ |
| $a, b, c$ (Å) | 10.200(1), 9.718(1), 5.5432(5) |
| $\beta$ (°) | 94.05(1)° |
| $V$ (Å³), Z | 548.1(1), 2 |
| $F(000)$ | 506 |
| $\mu$ (mm⁻¹) | 8.268 |
| Absorption correction | multi-scan |
| Crystal dimensions (mm) | $0.02 \times 0.03 \times 0.16$ |

**Data collection**

| | |
|---|---|
| Diffractometer | KAPPA APEX II |
| Temperature (K) | 293 |
| Radiation | Mo-$K\alpha$, $\lambda = 0.71073$ Å |
| $\theta$ range (°) | 2.00−30.94 |
| Detector distance (mm) | 37.5 |
| Rotation axes, width (°) | $\varphi, \omega, 2$ |
| Total no. of frames | 384 |
| Collection time per frame (s) | 120 |
| $h,k,l$ ranges | $-14 \rightarrow 14, -14 \rightarrow 14, -8 \rightarrow 6$ |
| Total reflections measured | 8874 |
| Unique reflections | 1726 ($R_{int} = 2.37\%$) |

**Refinement**

| | |
|---|---|
| Refinement on | $F^2$ |
| $R_1^*$ for $F_o > 4(F_o)$ | 1.60% |
| $wR_2^\dagger$ for all $F_o^2$ | 3.33% |
| Reflections used $[F_o^2 > 4\sigma(F_o^2)]$ | 1545 |
| Number of parameters refined | 114 |
| Extinction coefficient | 0.0006(4) |
| $(\Delta/\sigma)_{max}$ | 0.007 |
| $\Delta\rho_{min}, \rho_{max}$ (e/Å³) | −0.33, 0.48 |
| GoF | 1.061 |

* $R_1 = \Sigma||Fo|-|Fc||/\Sigma|Fo|$
† $wR_2 = \Sigma w(|Fo|^2-|Fc|^2)^2/\Sigma w|Fo|^2)^{1/2}$; $w = 1/[\sigma^2(F o^2) + (0.134 P)^2 + 0.2090 P]$;
$P = ([\text{max of } (0 \text{ or } F_0^2)] + 2Fc^2)/3$

type material, $a$ = 10.200(1), $b$ = 9.718(1), $c$ = 5.5432(5) Å, $\beta$ = 94.05(1)° and $V$ = 548.1(1) Å³, are very similar to those of the type material (minor differences are due to slightly different chemical compositions). Also, the $a{:}b{:}c$ axial ratio of the co-type material (1.050:1:0.570) is very similar to that of the type material (1.054:1:0.572). The material from Italy has the following, equally similar unit-cell parameters (refined from X-ray powder diffraction data, W. Krause, pers. comm. to U. Kolitsch, 2007): $a$ = 10.242(1), $b$ = 9.692(2), $c$ = 5.565(5) Å, $\beta$ = 94.18(3)° and $V$ = 550.9(2) Å³.

## Probable presence of vacancies and $Fe^{3+}$ in the Fe(I) site in bendadaite

A refinement of the structure of the phosphate analogue of bendadaite, whitmoreite, from film intensity data ($R_1$ = 14%; Moore *et al.*, 1974) showed that there are two independent Fe sites. The Fe(2) site contains only $Fe^{3+}$ whereas the Fe(1) site, assigned as $Fe^{2+}$, was found to be only partly occupied. On account of interatomic distance averages, Moore *et al.* (1974) assumed the presence of some trivalent Fe on this site and proposed the distribution Fe(1) = 0.58 (Fe, Mn)$^{2+}$ + 0.28 $Fe^{3+}$ + 0.14 vacancy.

TABLE 5. Fractional atomic coordinates and isotropic displacement parameters for co-type bendadaite.

| Atom | $x$ | $y$ | $z$ | $U_{eq}/U_{iso}$ | Occupancy |
|------|-----|-----|-----|------------------|-----------|
| Fe(1) | 0.0 | 0.0 | 0.0 | 0.01304(11) | $Fe^{2+}_{0.948(2)}$ |
| Fe(2) | 0.45715(2) | 0.13679(2) | 0.33999(4) | 0.00815(7) | $Fe^{3+}_{0.931(9)}Al_{0.040(18)}$ |
| As | 0.298182(17) | 0.426870(18) | 0.32898(3) | 0.00792(5) | $As_{0.741(6)}P_{0.263(15)}$ |
| O(1) | 0.39899(11) | 0.48388(11) | 0.11976(18) | 0.0122(2) | |
| O(2) | 0.35684(11) | 0.48686(11) | 0.59650(18) | 0.0137(2) | |
| O(3) | 0.15115(11) | 0.48741(12) | 0.2615(2) | 0.0179(3) | |
| O(4) | 0.29959(11) | 0.25662(12) | 0.32143(18) | 0.0140(2) | |
| Oh | 0.54491(11) | 0.23380(12) | 0.08027(19) | 0.0140(2) | |
| Ow(1) | 0.12925(14) | −0.09593(14) | 0.2979(2) | 0.0241(3) | |
| Ow(2) | 0.04589(16) | 0.18779(15) | 0.1498(3) | 0.0298(3) | |
| H | 0.586(2) | 0.176(3) | 0.999(4) | 0.039(7) | |
| H11 | 0.208(3) | 0.915(3) | 0.262(5) | 0.057(9) | |
| H12 | 0.128(3) | 0.941(3) | 0.456(5) | 0.056(8) | |
| H21 | 0.118(3) | 0.211(3) | 0.226(5) | 0.061(9) | |
| H22 | 0.992(3) | 0.247(3) | 0.181(5) | 0.057(9) | |

Oxygens of the hydroxyl group are designated as Oh, those of $H_2O$ molecules as Ow.

Our study suggests that in bendadaite the Fe(1) site is also not fully occupied, but that a mixture of major $Fe^{2+}$, minor $Fe^{3+}$, very small amounts of Mn, Zn and Ca, and vacancies is present on this site. Corresponding to the situation in whitmoreite, the distribution Fe(1) = 0.52 $Fe^{2+}$ + 0.32 $Fe^{3+}$ + 0.16 vacancy is considered likely, corresponding to the formula $(Fe^{2+}_{0.52}Fe^{3+}_{0.32}\square_{0.16})_{\Sigma 1.00}$ $(Fe^{3+}_{1.89}Al_{0.11})_{\Sigma 2.00}(As_{1.87}P_{0.13})_{\Sigma 2.00}O_8$ $(OH)_{2.00}\cdot4H_2O$, i.e. with an ideal hydroxyl content.

From a structure refinement of an ojuelaite crystal (the Zn analogue of bendadaite) containing excess iron, Hughes *et al.* (1996) derived the formula $(Zn_{0.77}Fe_{0.23})_{\Sigma 1.00}Fe^{3+}_{2.00}(AsO_4)_{1.94}$ $(OH)_2\cdot3.75H_2O$ based on electron microprobe analyses (water by difference). These results indicate that no vacancies were present in (this) ojuelaite. Hughes *et al.* (1996) stated that it is not known if the iron, which is substituting for Zn, is only $Fe^{2+}$, or if it is $Fe^{3+}$ that is charge-balanced by a mechanism such as a concomitant $O \rightleftharpoons (OH)$ substitution. However, a single-crystal structure refinement of cobaltarthurite (from Morocco), the Co analogue of bendadaite (Kampf, 2005), showed that the (Co, Fe) site is not fully occupied

TABLE 6. Anisotropic displacement parameters for bendadaite (co-type locality).

| Atom | $U_{11}$ | $U_{22}$ | $U_{33}$ | $U_{23}$ | $U_{13}$ | $U_{12}$ |
|------|----------|----------|----------|----------|----------|----------|
| Fe(1) | 0.01469(18) | 0.01264(18) | 0.01210(17) | −0.00171(11) | 0.00241(11) | −0.00285(13) |
| Fe(2) | 0.01042(12) | 0.00689(12) | 0.00716(11) | 0.00007(7) | 0.00074(7) | 0.00032(8) |
| As | 0.00861(9) | 0.00787(9) | 0.00738(8) | 0.00012(6) | 0.00130(5) | 0.00010(6) |
| O(1) | 0.0136(5) | 0.0117(5) | 0.0116(5) | −0.0014(4) | 0.0025(4) | −0.0013(4) |
| O(2) | 0.0166(6) | 0.0126(6) | 0.0117(5) | 0.0010(4) | −0.0010(4) | −0.0005(4) |
| O(3) | 0.0161(6) | 0.0207(6) | 0.0170(5) | 0.0016(4) | 0.0028(4) | 0.0015(5) |
| O(4) | 0.0160(6) | 0.0125(6) | 0.0136(5) | −0.0004(4) | 0.0007(4) | 0.0026(4) |
| Oh | 0.0167(6) | 0.0130(6) | 0.0124(5) | 0.0026(4) | 0.0033(4) | 0.0034(4) |
| Ow(1) | 0.0213(7) | 0.0304(8) | 0.0205(6) | −0.0015(5) | 0.0002(5) | −0.0039(5) |
| Ow(2) | 0.0248(8) | 0.0224(7) | 0.0420(8) | −0.0145(6) | 0.0008(6) | −0.0031(6) |

TABLE 7. Selected bond distances (Å) for the coordination polyhedra in co-type bendadaite.

| | | | |
|---|---|---|---|
| Fe(1)−Ow(2) × 2 | 2.0456(14) | Fe(2)−O(4) | 1.9815(11) |
| −O(3) × 2 | 2.1043(11) | −Oh | 1.9861(11) |
| −Ow(1) × 2 | 2.2418(13) | −Oh | 1.9971(11) |
| <Fe(1)−O> | 2.131 | −O(2) | 2.0292(11) |
| | | −O(1) | 2.0645(11) |
| As−O(3) | 1.6298(12) | −O(1) | 2.0893(11) |
| −O(4) | 1.6551(12) | <Fe(2)−O> | 2.025 |
| −O(2) | 1.6648(11) | | |
| −O(1) | 1.6963(11) | | |
| <As−O> | 1.662 | | |

| | Hydrogen bonds[1] | | |
|---|---|---|---|
| Oh−H | 0.85 | Oh−H···O(2) | 2.80 |
| Ow(1)−H(11) | 0.85 | Ow(1)−H(11)···O(2) | 2.85 |
| Ow(1)−H(12) | 0.95 | Ow(1)−H(12)···O(3) | 2.77 |
| Ow(2)−H(21) | 0.85 | Ow(2)−H(21)···O(4) | 2.78 |
| Ow(2)−H(22) | 0.82 | Ow(2)−H(22)···Ow(1) | 2.78 |

[1] O−H distances were refined without restraints.
O−H−O angles range between 156 and 172°.



FIG. 6. View along the $c$ axis of the crystal structure of co-type bendadaite (unit-cell is outlined). The Fe(1)$O_6$ octahedra connect the sheets composed of corner-sharing Fe(2)$O_6$ octahedra and AsO$_4$ tetrahedra. Weak hydrogen bonds (not shown) provide further strengthening of the framework.

(occupancy 0.93), although it is filled to a greater extent than indicated by EPMA data (occupancy 0.77). The original description of cobaltarthurite (type material from Spain; Jambor et al., 2002) suggested a similar occupancy of 0.93, whereas a Rietveld refinement and re-analysis of the type material indicated full occupancy (Raudsepp and Pani, 2002).

The possibility that all iron in bendadaite is trivalent can be ruled out on account of the positive microchemical test for $Fe^{2+}$ and the thermal studies (see below). In this respect, it is noteworthy that for whitmoreite, the phosphate analogue of bendadaite with the formula $Fe^{2+}Fe_2^{3+}(PO_4)_2(OH)_2 \cdot 4H_2O$, an oxidized variety was reported from the Hagendorf pegmatite, Bavaria, Germany (Mücke, 1981; Kastning and Schlüter, 1994, p. 49). It is found in altered rockbridgeite and forms lemon-yellow, opaque radiating aggregates, whereas unoxidized whitmoreite is brown. In this oxidized variety, the Fe(1) site may be occupied by dominant $Fe^{3+}$ (the oxidation also possibly being affected by the loss of water and/or the transformation of some water into hydroxyl according to the reaction scheme $Fe^{2+} + H_2O \rightarrow Fe^{3+} + OH^-$). A similarly oxidized variety of bendadaite may exist in nature; it would have the hypothetical end-member formula $Fe_3^{3+}(AsO_4)_2(OH)_3 \cdot 3H_2O$.

Partial occupation of di-/trivalent Fe-sites in Fe phosphates and associated variable $Fe^{2+}/Fe^{3+}$ ratios are known from several mineral species (e.g. rockbridgeite, lipscombite; Moore, 1970) and also from synthetic compounds such as $Fe^{2+}Fe_2^{3+}(PO_3OH)_4(H_2O)_4$ (Vencato et al., 1986). Therefore, the partial occupation of the Fe(2) site (assumed to be occupied completely by $Fe^{3+}$ only, in the ideal formula) obviously cannot be ruled out, although charge-balance considerations make it appear less likely.

The macroscopic colour of bendadaite and its optical absorption colours shown under polarized light strongly indicate $Fe^{2+}$-$Fe^{3+}$ charge transfer colouring, but also suggest an at least partial oxidation of $Fe^{2+}$ to $Fe^{3+}$ (iron phosphates containing both $Fe^{2+}$ and $Fe^{3+}$ commonly have a dark greenish colour whereas more or less oxidized varieties of these minerals show brownish, orangish and reddish colours; Moore, 1970). These conclusions, of course, ignore any possible influence of the As and the impurity cations on the colours. According to Moore et al. (1974), the structurally analogous whitmoreite is characterized by corner- and edge-shared

$Fe^{3+}(O,OH)_6$ octahedra forming sheets parallel to {100}, with $Fe^{2+}$-$(OH_2,O)$ polyhedra between the sheets. The pale reddish brown absorption colour approximately parallel to [010] observed for X of bendadaite corresponds to the reddish brown colour typical of some silicate minerals showing $Fe^{2+}$-$Fe^{3+}$ charge transfer colouring (e.g. hypersthene, hornblende, biotite and staurolite).

## Conditions of formation

As stated previously, while most of the bendadaite aggregates are overgrown by a scorodite–mansfieldite crust, only rarely is bendadaite itself grown on scorodite–mansfieldite. This relationship suggests that bendadaite was formed more or less contemporaneously with scorodite–mansfieldite as a direct weathering product of the closely associated arsenopyrite. The co-existence with the secondary ferric/aluminum arsenate scorodite–mansfieldite indicates a low-temperature, oxidizing environment favouring the oxidation of $Fe^{2+}$ to $Fe^{3+}$ (according to Vink (1996), scorodite also crystallizes at moderate to high Eh). As scorodite was found to form at a pH of ~1–6 from highly concentrated solutions of $Fe^{3+}$ and $AsO_4^{3-}$ (Dove and Rimstidt, 1985; Rimstidt and Dove, 1987; Dutrizac & Jambor, 1988; Krause and Ettel, 1988; Le Berre et al., 2007; Paktunc et al., 2008), it may be assumed that bendadaite forms under similar conditions. It is interesting to note that arthurite, the $Cu$-$Fe^{3+}$-arsenate end-member of the arthurite group, was found to commonly co-exist with scorodite (e.g. Davis and Hey, 1964; Walenta, 1975; Jensen, 1985, 1993; Blaß and Helsper, 1994).

In the Kamariza mines, Lavrion, Greece, an intermediate member of the bendadaite–ojuelaite series with the empirical formula $(Zn_{0.52}Fe_{0.34} Mg_{0.10}\square_{0.04})_{\Sigma 1.00}Fe_{2.00}^{3+}(As_{1.97}P_{0.03})_{\Sigma 2.00} O_8(OH)_2 \cdot nH_2O$ was discovered by the present authors in association with scorodite.

At the Bendada pegmatite occurrence, arthurite and whitmoreite were also found (Schnorrer-Köhler and Rewitzer, 1991); whitmoreite was observed in a completely different paragenesis, with several other phosphates.

The conditions of formation of bendadaite and its thermodynamic stability field appear to be restricted, with an equilibrium between $Fe^{2+}$ and $Fe^{3+}$ oxidation states being necessary. The observed Al, Mn and P impurities in most samples seem to help to stabilize the bendadaite.

## References

Allen, V.T., Fahey, J.J. and Axelrod, J.M. (1948) Mansfieldite, a new arsenate, the aluminum analogue of scorodite, and the mansfieldite−scorodite series. *American Mineralogist*, **33**, 122−134.

Blaß, G. and Helsper, G. (1994) The "Sophie" mine near Gosenbach in the Siegerland and its minerals. *Mineralien-Welt*, **5** (6), 40−47 (in German).

Brese, N.E. and O'Keeffe, M. (1991) Bond-valence parameters for solids. *Acta Crystallographica*, **B 47**, 192−197.

Cesbron, F., Romero, S.M. and Williams, S.A. (1981) La mapimite et l'ojuélaïte, deux nouveaux arséniates hydratés de zinc et de fer de la mine Ojuela, Mapimi, Mexique. *Bulletin de Minéralogie*, **104**, 582−586.

Clark, A.H. and Sillitoe, R.H. (1969) Arthurite from Potrerillos, Atacama Province, Chile. *Mineralogical Magazine*, **37**, 519−520.

Correia Neves, J.M. (1960) Pegmatitos com berilo, columbite-tantalite e fosfatos da Bendada (Sabugal, Guarda). *Memórias e Notícias, Museu e Laboratório Mineralógico e Geológico da Universidade de Coimbra, Coimbra*, **50**, 163 pp. (in Portuguese).

Dasgupta, D.R., Datta, A.K. and Sen Gupta, N.R. (1966) Occurrence of scorodite in a pegmatite in Bhilwara district, Rajasthan, India. *Mineralogical Magazine*, **35**, 776−777.

Davis, R.J. and Hey, M.H. (1964) Arthurite, a new copper-iron arsenate from Cornwall. *Mineralogical Magazine*, **33**, 937−941.

Davis, R.J. and Hey, M.H. (1969) The cell-contents of arthurite redetermined. *Mineralogical Magazine*, **37**, 520−521.

Dove, P.M. and Rimstidt, J.D. (1985) The solubility and stability of scorodite, $FeAsO_4 \cdot 2H_2O$. *American Mineralogist*, **70**, 838−844.

Dutrizac, J. E. and Jambor, J. L. (1988) The synthesis of crystalline scorodite, $FeAsO_4 \cdot 2H_2O$. *Hydrometallurgy*, **19**, 377−384

Favreau, G. and Dietrich, J.E. (2006) The minerals of Bou Azzer. *Lapis*, **31** (7−8), 27−68 (in German).

Frost, R.L., Duong, L. and Martens, W. (2003) Molecular assembly in secondary minerals Raman spectroscopy of the arthurite group species, arthurite and whitmoreite. *Neues Jahrbuch für Mineralogie, Monatshefte*, **2003**, 223−240.

Hughes, J.M., Bloodaxe, E.S., Kobel, K.D. and Drexler, J.W. (1996) The atomic arrangement of ojuelaite, $ZnFe_2^{3+}(AsO_4)_2(OH)_2 \cdot 4H_2O$. *Mineralogical Magazine*, **60**, 519−21.

Jambor, J.L., Viñals, J., Groat, L.A. and Raudsepp, M. (2002) Cobaltarthurite, $Co^{2+}Fe_2^{3+}(AsO_4)_2(OH)_2 \cdot 4H_2O$, a new member of the arthurite group. *The Canadian Mineralogist*, **40**, 725−732.

Jensen, M. (1985) The Majuba Hill mine, Pershing County. *Mineralogical Record*, **16**, 57−72.

Jensen, M. (1993) Update on the mineralogy of the Majuba Hill mine, Pershing County. *Mineralogical Record*, **24**, 171−180.

Kampf, A.R. (2005) The crystal structure of cobalt-arthurite from the Bou Azzer District, Morocco: the location of hydrogen atoms in the arthurite structure-type. *The Canadian Mineralogist*, **43**, 1387−1391.

Kampf, A.R., Favreau, G. and Steele, J. M. (2004) Cobaltarthurite from the Bou Azzer district, Morocco. *5th International Conference on Mineralogy and Museums. Paris, France, September 6−8, 2004, Program and abstract volume*, p. 40.

Kastning, J. and Schlüter, J. (1994) *The Minerals of Hagendorf and their Identification*. Schriften des Mineralogischen Museums der Universität Hamburg, Band 2, C. Weise Verlag, Munich, Germany (in German).

Keller, P. and Hess, H. (1978) Die Kristallstruktur von Arthurit, $CuFe_2^{3+}[(H_2O)_4|(OH)_2|(AsO_4)_2]$. *Neues Jahrbuch für Mineralogie, Abhandlungen*, **133**, 291−302.

Krause, E. and Ettel, V.A. (1988) Solubility and stability of scorodite, $FeAsO_4 \cdot 2H_2O$: New data and further discussion. *American Mineralogist*, **73**, 850−854.

Le Berre, J.F., Cheng, T.C., Gauvin, R. and Demopoulos, G.P. (2007) Hydrothermal synthesis and stability evaluation of mansfieldite in comparison to scorodite. *Canadian Metallurgical Quarterly*, **46**, 1−10.

Mandarino, J.A. (1981) The Gladstone-Dale relationship: Part IV. The compatibility concept and its application. *The Canadian Mineralogist*, **19**, 441−450.

Mills, S.J., Kolitsch, U., Birch, W.D. and Sejkora, J. (2008) Kunatite, $CuFe_2^{3+}(PO_4)_2(OH)_2 \cdot 4H_2O$, a new member of the whitmoreite group, from Lake Boga, Victoria, Australia. *Australian Journal of Mineralogy*, **14**, 3−12.

Moore, P.B. (1970) Crystal chemistry of the basic iron phosphates. *American Mineralogist*, **55**, 135−169.

Moore, P.B., Kampf, A.R. and Irving, A.J. (1974) Whitmoreite, $Fe^{2+}Fe_2^{3+}(OH)_2(H_2O)_4[PO_4]_2$, a new species: Its description and atomic arrangement. *American Mineralogist*, **59**, 900−905.

Mücke, A. (1981) The parageneses of the phosphate minerals of the Hagendorf pegmatite − a general view. *Chemie der Erde*, **40**, 217−234.

Paktunc, D., Dutrizac, J. and Gertsman, V. (2008) Synthesis and phase transformations involving scorodite, ferric arsenate and arsenical ferrihydrite: Implications for arsenic mobility. *Geochimica et Cosmochimica Acta*, **72**, 2649−2672.

Peacor, D.R., Dunn, P.J. and Simmons, W.B. (1984) Earlshannonite, the Mn analogue of whitmoreite, from North Carolina. *The Canadian Mineralogist*, **22**, 471−474.

Raudsepp, M. and Pani, E. (2002) The crystal structure of cobaltarthurite, $Co^{2+}Fe_2^{3+}(AsO_4)_2(OH)_2 \cdot 4H_2O$, a Rietveld refinement. *The Canadian Mineralogist*, **40**, 733−737.

Rewitzer, C. and Röschl, N. (1984) Portugal − locality descriptions and travel recommendations. *Lapis*, **9** (12), 13−17 (in German).

Rimstidt, J.D. and Dove, P.M. (1987) Solubility and stability of scorodite, $FeAsO_4 \cdot 2H_2O$: Reply. *American Mineralogist*, **72**, 852−855.

Schnorrer-Köhler, G. and Rewitzer, Chr. (1991) Bendada − a phosphate pegmatite in the middle part of Portugal. *Lapis*, **16** (5), 21−33 (in German).

Sejkora, J., Škoda, R. and Ondruš, P. (2006) New naturally occurring mineral phases from the Krásno Horní Slavkov area, western Bohemia, Czech Republic. *Journal of the Czech Geological Society*, **51**, 159−187.

Shannon, R.D. (1976) Revised effective ionic radii and systematic studies of interatomic distances in halides and chalcogenides. *Acta Crystallographica*, **A32**, 751−767.

Sheldrick, G.M. (2008) A short history of *SHELX*. *Acta Crystallographica*, **A64**, 112−122.

Vencato, I., Mascarenhas, Y.P. and Mattievich, E. (1986) The crystal structure of $Fe^{2+}Fe_2^{3+}(PO_3OH)_4(H_2O)_4$: a new synthetic compound of mineralogical interest. *American Mineralogist*, **71**, 222−226.

Vink, B.W. (1996) Stability relations of antimony and arsenic compounds in the light of revised and extended Eh-pH diagrams. *Chemical Geology*, **130**, 21−30.

Walenta, K. (1963) Mansfieldite from Neubulach in the Württemberg Black Forest. *Neues Jahrbuch für Mineralogie, Monatshefte*, **1963**, 79−87 (in German).

Walenta, K. (1975) The secondary minerals of the barite vein of the Clara mine near Oberwolfach, central Black Forest. *Aufschluss*, **26**, 369−311 (in German).

Yvon, K., Jeitschko, W. and Parthé, E. (1977) LAZY PULVERIX, a computer program, for calculating X-ray and neutron diffraction powder patterns. *Journal of Applied Crystallography*, **10**, 73−74.